Acta Biomaterialia xxx (2017) xxx–xxx

Contents lists available at ScienceDirect

Acta Biomaterialia

journal homepage: www.elsevier.com/locate/actabiomat

Full length article

Dragonfly wing nodus: A one-way hinge contributing to the asymmetric wing deformation

H. Rajabi [a,*], N. Ghoroubi [b,1], K. Stamm [a,1], E. Appel [a], S.N. Gorb [a]

[a] Institute of Zoology, Functional Morphology and Biomechanics, Kiel University, Kiel, Germany
[b] Young Researchers and Elite Club, Rasht Branch, Islamic Azad University, Rasht, Iran

ARTICLE INFO

Article history:
Received 23 May 2017
Received in revised form 18 July 2017
Accepted 20 July 2017
Available online xxxx

Keywords:
Dragonfly wing
Nodus
Resilin
Interlocking
Asymmetric deformation
Numerical modelling

ABSTRACT

Dragonfly wings are highly specialized locomotor systems, which are formed by a combination of several structural components. The wing components, also known as structural elements, are responsible for the various aspects of the wing functionality. Considering the complex interactions between the wing components, modelling of the wings as a whole is only possible with inevitable huge oversimplifications. In order to overcome this difficulty, we have recently proposed a new approach to model individual components of complex wings comparatively. Here, we use this approach to study nodus, a structural element of dragonfly wings which has been less studied to date. Using a combination of several imaging techniques including scanning electron microscopy (SEM), wide-field fluorescence microscopy (WFM), confocal laser scanning microscopy (CLSM) and micro-computed tomography (micro-CT) scanning, we aim to characterize the spatial morphology and material composition of fore- and hindwing nodi of the dragonfly *Brachythemis contaminata*. The microscopy results show the presence of resilin in the nodi, which is expected to help the deformability of the wings. The computational results based on three-dimensional (3D) structural data suggest that the specific geometry of the nodus restrains its displacements when subjected to pressure on the ventral side. This effect, resulting from an interlocking mechanism, is expected to contribute to the dorso-ventral asymmetry of wing deformation and to provide a higher resistance to aerodynamic forces during the downstroke. Our results provide an important step towards better understanding of the structure–property-function relationship in dragonfly wings.

Statement of Significance

In this study, we investigate the wing nodus, a specialized wing component in dragonflies. Using a combination of modern imaging techniques, we demonstrate the presence of resilin in the nodus, which is expected to facilitate the wing deformability in flight. The specific geometry of the nodus, however, seems to restrain its displacements when subjected to pressure on the ventral side. This effect, resulting from an interlocking mechanism, is suggested to contribute to dorso-ventral asymmetry of wing deformations and to provide a higher resistance to aerodynamic forces during the downstroke. Our results provide an important step towards better understanding of the structure–property-function relationship in dragonfly wings and might help to design more efficient wings for biomimetic micro-air vehicles.

1. Introduction

Dragonflies are one of the most sophisticated flyers in the natural world [1]. The superior flight characteristics exhibited by these insects can rarely be found in other flying insects [2]. The skilful flight of dragonflies is believed to be mainly the result of the unique architecture of their wings [3–5]. The wings consist of several major components, which contribute to their deformations during flight [3–8]. These deformations are expected to remarkably influence the aerodynamic performance of the wings, and consequently the flight style of the insects [9,10].

According to their functions, the structural components of a dragonfly wing can be divided into two main groups: (i) supporting and (ii) mobilizing elements. Supporting elements are those which provide support for the wing and stiffen its structure against buckling, bending and twisting. Thickened areas [5], veins [11], membrane [12], fused microjoints [3,13,14] and joint-associated

* Corresponding author.
E-mail addresses: hrajabi@zoologie.uni-kiel.de, harajabi@hotmail.com (H. Rajabi).
[1] Both these authors have contributed equally to this work.

http://dx.doi.org/10.1016/j.actbio.2017.07.034
1742-7061/

spikes [3,13,14] are some of these supporting elements. In contrast, mobilizing elements are those which improve the wing deformability. These elements are believed to play an important role in dragonfly flight by increasing the aerodynamic lift generation [15]. Vein fractures [16], flexion lines [16], resilin patches [17] and resilin microjoints [7,18] can be considered as mobilizing elements.

There are also some other wing components that can be included in both groups. One example is the wing corrugation. The corrugated pattern increases the flexural stiffness of the wing, but on the other hand facilitates its torsional deformability [19]. Leading edge spar [10], basal complex [10,20], and vein ultrastructure [6,21] are three other wing components with essentially the same function as that of the wing corrugation.

In comparison to the other wing components, there are only few data in the literature regarding the role of the nodus in the wing deformability [3,10,22]. The present data indicate that the nodus is a marked structure in the leading edge spar (Fig. 1A), which separates it into two parts (the proximal or pre-nodal and the distal or post-nodal parts). In dragonflies, the nodus typically lies between 47% and 60% of the forewing span [4]. However, in their hindwings, it has been a bit shifted to the base and is located at 40% to 46% of the wing span.

The mechanical function of the nodus was first proposed by Norberg [22]. Although no concrete evidence was given, he suggested that the nodus permits strong wing twisting during the up- and downstrokes, and further plays a role as a "shock absorber". Later, Newman [3] and recently Fauziyah et al. [23] demonstrated the presence of soft cuticle in the break of the costal vein, an observation that could provide support for Norberg's hypothesis.

Using the available data, it is still difficult to unambiguously categorize the nodus in either of the previously mentioned groups. Considering this, the present study is designed to provide detailed biomechanical data on the three-dimensional (3D) configuration and material composition of the nodus of dragonfly wings by means of modern imaging techniques. Furthermore, using sets of numerical models, we show how the observed characteristics may affect the functionality of the nodus. The aim is certainly not to reproduce the real wing deformations, but to provide a comparative study demonstrating the potential influence of the nodus on the deformability of dragonfly wings.

2. Materials and methods

2.1. Sample preparation

Specimens of the dragonfly *Brachythemis contaminata* (Anisoptera, Libellulidae) were collected in Nanjing (China) in August 2015 (Fig. 1A). They were euthanized using CO_2 gas and dried at room temperature. Three male insects with relatively similar sizes were selected for this study. The wings were carefully removed from the bodies using sharp razor blades.

2.2. Wide-field fluorescence microscopy

A well-known characteristic of insect cuticle is its autofluorescence at different wavelengths, when excited with UV-light [24–26]. This characteristic can be used to determine the material composition of the cuticle, especially its degree of sclerotization and

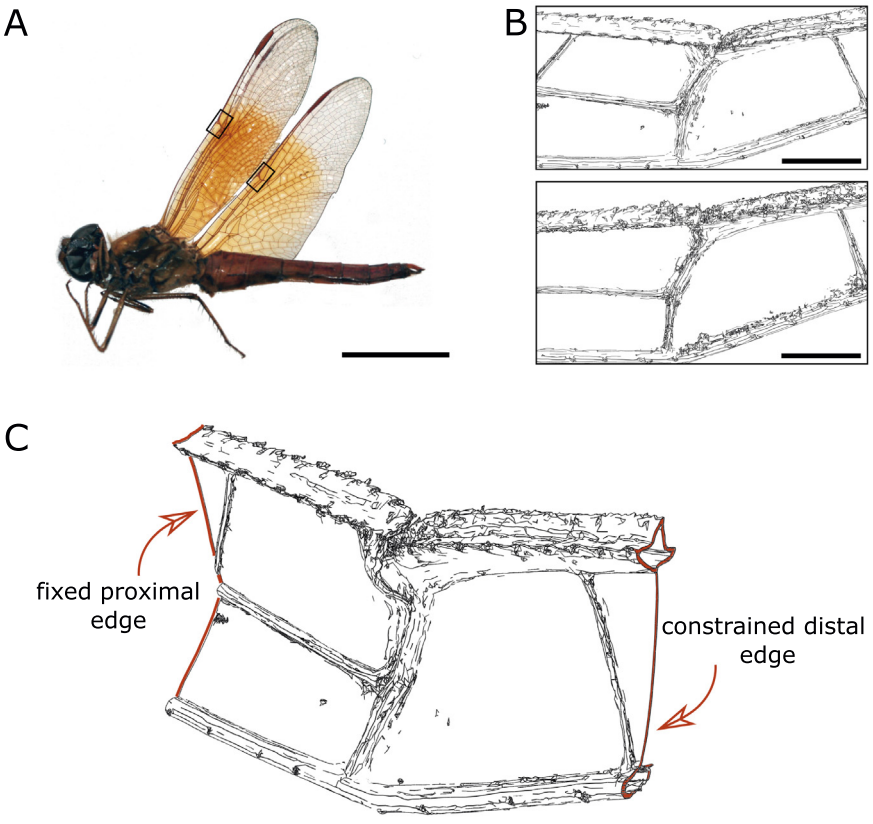

Fig. 1. (A) The dragonfly *B. contaminata*. The black rectangles on the wings show the parts of the wings investigated in this study, the nodi. (B) Developed models of the fore- and hindwing nodi. The images have been generated using the FE software package ABAQUS. (C) Before FE analysis, the models were fixed at the extreme proximal edge and a tie constraint was used to bond their extreme distal edge to a reference point set on the aerodynamic pressure centre of the wings. Scale bars: 1 cm (A), 0.5 mm (B).

Please cite this article in press as: H. Rajabi et al., Dragonfly wing nodus: A one-way hinge contributing to the asymmetric wing deformation, Acta Biomater. (2017), http://dx.doi.org/10.1016/j.actbio.2017.07.034

the presence of resilin [25,27]. As shown by [28], resilin has excitation and emission maxima of around 320 nm and 415 nm (in neutral solutions), respectively, but can also be successfully visualized by using higher excitation wavelengths at the outer borders of the spectrum [25]. Sclerotized cuticle was shown to be dominated by red autofluorescence, whereas less sclerotized, more chitinous cuticle has a mainly green autofluorescence.

Wide-field fluorescence microscopy (WFM) was employed to assess the occurrence of resilin in the wing nodus. For this purpose, the fore- and hindwing samples were first rehydrated for 24 h. Then, they were shortly washed with 70% ethanol and mounted in glycerine between a glass slide and a cover slip. A fluorescence microscope (Zeiss Axioplan, Oberkochen, Germany) equipped with a DAPI-filter set (excitation 321–378, FT395, BP420–470 nm) was utilized to observe both dorsal and ventral sides of the nodus of both wings.

2.3. Confocal laser scanning microscopy

Michels and Gorb [25] showed that a confocal laser scanning microscope equipped with a 405 nm laser can be employed to demonstrate the presence of resilin in insect exoskeleton. Confocal laser scanning microscopy (CLSM) has been also demonstrated to be a useful technique to gain a detailed understanding of the material distribution in biological structures [25,27,29].

Considering the similarity of the preparation methods, the same specimens used in WFM were tested in CLSM. The confocal laser scanning microscope (Zeiss LSM 700, Carl Zeiss Microscopy, Jena, Germany) employed in this study had four stable solid-state lasers with wavelengths of 405 nm, 488 nm, 555 nm and 639 nm. The following emission filters were utilized to detect autofluorescence emitted from the nodus: BP420–480, LP490, LP560 and LP640 nm.

2.4. Micro-computed tomography

A Skyscan 1172 micro-computed tomography (micro-CT) scanner (Bruker microCT, Kontich, Belgium) was employed to investigate the 3D configuration of the nodus. For this purpose, small parts of fore- and hindwings containing the nodus (~3 mm length) were cut and fixed on the sample stage of the micro-CT scanner. The samples were scanned with a resolution of about 1 μm at a source voltage of 40 kV and a current of 250 μA. The data from

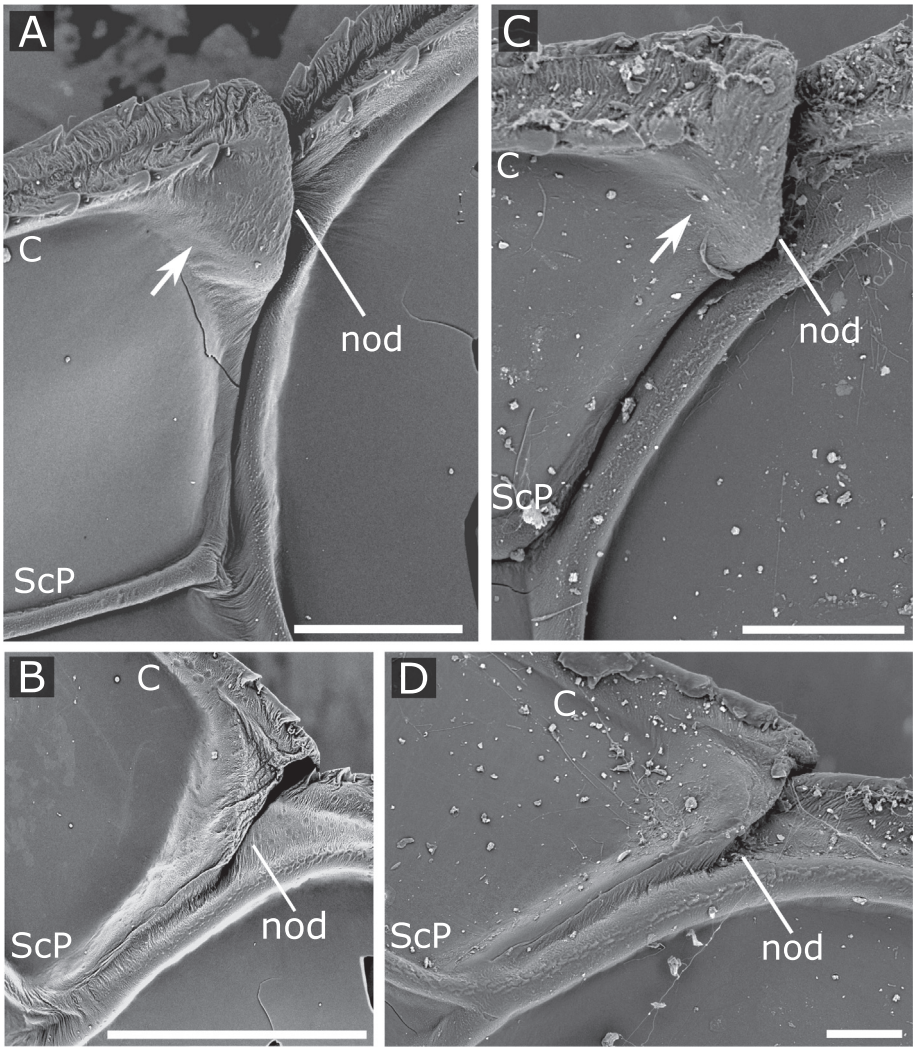

Fig. 2. SEM images of the fore- and hindwing nodi of the dragonfly *B. contaminata*. (A) Dorsal side of the forewing nodus, representing the interface of the pre- and post-nodal parts. The costal and subcostal veins are located on the pre-nodal part of the nodus. The elevated ridge (white arrow) is located on the distal end of the costal vein in the proximal part of the nodus and somewhat covers its distal part. (B) Ventral side of the forewing nodus. The break between the pre-nodal and post-nodal parts of the costal vein and the interface of the pre- and post-nodal parts can be seen here. It seems that ScP makes a transition to the post-nodal region of the leading edge spar. (C) Dorsal side of the hindwing nodus representing the elevated ridge, break and transition between the costal and subcostal veins. (D) Ventral side of the hindwing nodus. The break between the pre-nodal and post-nodal parts of the costal veins is shown here. The pre-nodal and post-nodal parts of the nodus can be found in the left- and right-hand side of each image, respectively. nod, nodus; C, Costal vein (Costa); ScP, posterior subcostal vein. Scale bars: 500 μm (A, B), 200 μm (C), 100 μm (D).

Please cite this article in press as: H. Rajabi et al., Dragonfly wing nodus: A one-way hinge contributing to the asymmetric wing deformation, Acta Biomater. (2017), http://dx.doi.org/10.1016/j.actbio.2017.07.034

the scans were reconstructed in the NRecon reconstruction software package (SkyScan, Kontich, Belgium). 3D image analysis software Amira (FEI Visualization Sciences Group, Bordeaux, France) was utilized for developing finite element (FE) models of the nodus based on the reconstructed data.

2.5. Scanning electron microscopy

The same specimens used in micro-CT scanning were used later for scanning electron microscopy (SEM). The small wing parts were mounted on sample holders using carbon Leit-tabs (Plano GmbH, Wetzlar, Germany). A Leica EM SCD 500 high-vacuum sputter coater (Leica Microsystems, Mannheim, Germany) was used to coat them with a thin layer of gold-palladium alloy (~9 nm). The specimens were imaged using a Hitachi S-4800 scanning electron microscope (Hitachi High-Tech., Tokyo, Japan) at an accelerating voltage of 3 kV.

2.6. Numerical analysis

The 3D visualization software package Amira v6.0 (FEI SAS, Mérignac Cedex, France) was used to develop FE models based on the data obtained from the micro-CT scanning. Several models with varying number of elements were created for both fore- and hindwings, which allowed to perform a mesh convergence analysis later on. The models were then exported to Materialise Magics STL editor software (Materialise, Leuven, Belgium) to check and fix their potential errors, especially intersecting elements, bad edges and holes. After this adjustment, the commercial FE software package ABAQUS/Standard v6.14 (Simulia, Providence, RI) was utilized to convert the two-dimensional (2D) shell elements of the models (created by Amira) to volumetric ones. The models were meshed using general purpose tetrahedral elements (C3D10), which are recommended for structural analyses similar to that presented in this study [30]. The second-order interpolation of these elements leads to a higher accuracy of the results, compared to when linear elements are employed.

We have previously shown that the mechanical behaviour of insect wings can be estimated using a linear elastic material model [8,9,13,14,20,21,31,32]. Here, we used the same method to simulate the mechanical response of the nodus to external forces applied during flight. For this purpose, a stiffness and a Poisson's ratio of 3 GPa [33] and 0.49 [11], respectively, were assigned to the models. The Young's modulus of resilin was considered to be 2 MPa [29].

In order to capture the effect of changes in the geometric configuration of the models resulting from possible large deformations, a geometric nonlinear analysis was carried out. The large deforma-

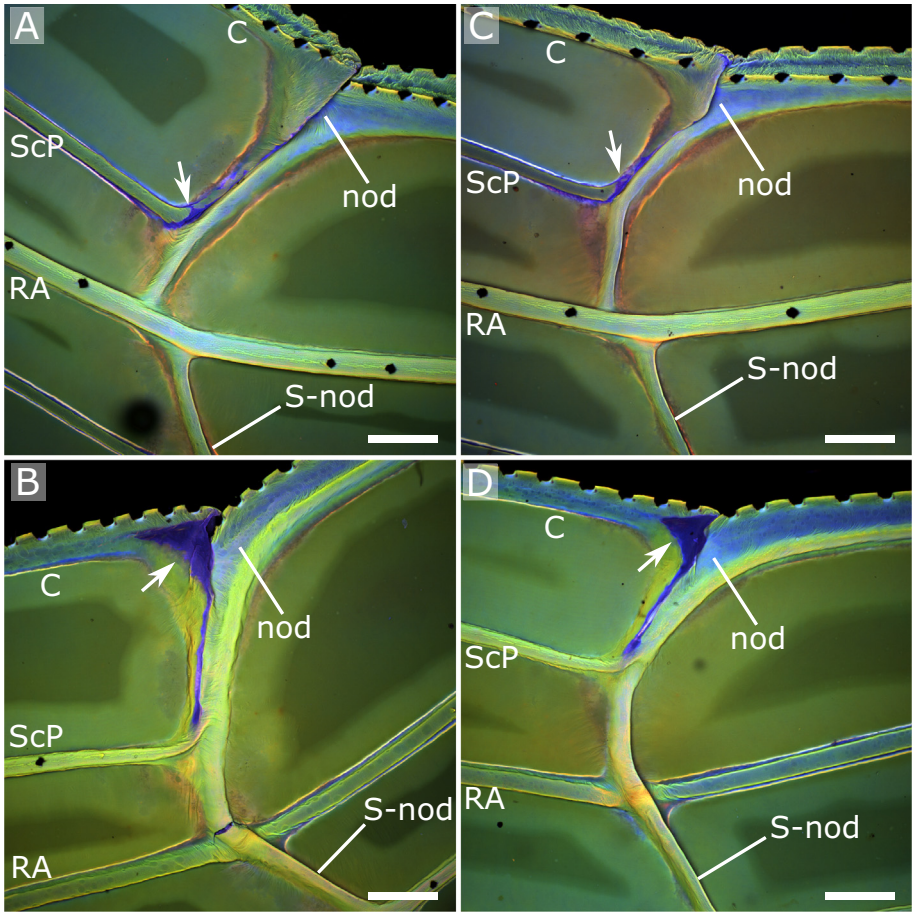

Fig. 3. CLSM images of the fore- and hindwing nodi of the dragonfly *B. contaminata*. The presence of the blue, green and red colours indicates the presence of resilin, less-sclerotized and highly-sclerotized cuticle, respectively. (A) Dorsal and (B) ventral sides of the forewing nodus. (C) Dorsal and (D) ventral sides of the hindwing nodus. Resilin in both wings can be mainly found in the interface of the pre- and post-nodal parts and also in the transition of the costal and subcostal veins on the dorsal side. The pre-nodal and post-nodal parts of nodus can be found in the left- and right-hand side of each image, respectively. nod, nodus; S-nod, sub-nodus; C, Costal vein (Costa); ScP, posterior subcostal vein; RA, anterior radial vein. Scale bars: 200 μm. (For interpretation of the references to colour in this figure legend, the reader is referred to the web version of this article.)

Please cite this article in press as: H. Rajabi et al., Dragonfly wing nodus: A one-way hinge contributing to the asymmetric wing deformation, Acta Biomater. (2017), http://dx.doi.org/10.1016/j.actbio.2017.07.034

tions may also cause the different parts of the models to come in contact. Therefore, we conducted a self-contact analysis to consider the possible interactions between the parts of our models.

The ABAQUS implicit solver was used to simulate the mechanical behaviour of the nodus subjected to an applied force. For this purpose, all displacements and rotations of the extreme proximal end of the models were constrained to be zero (Fig. 1C). On the other side, a tie constraint was used to bond the extreme distal end of the models to a reference point set on the aerodynamic pressure centre of the wings. The defined tie constraint eliminates the degrees of freedom of the free end of the models and couples its motion to that of the reference point. This reference point was then subjected to a concentrated force which is assumed to be equal to a portion of the aerodynamic force applied to the region of the insect wings considered in our models.

It has been previously shown that the bending and torsional moments induced by aerodynamic forces during flight are predominantly carried by longitudinal veins [8]. There are eight main longitudinal veins in the wings of the dragonfly *B. contaminata*, of which two of them forming the nodus (costal and radial veins) are included in our models (Fig. 1B). Therefore, assuming the same aerodynamic lift generation by the wings, we can expect that the part of the wings modelled in our study is subjected to an aerodynamic force almost equal to 12% of the insect body weight (0.103 mN) when in hovering flight [34]. The aerodynamic forces applied to the models during take-off and gliding were taken to be 2.5 times [35] and 0.3 times [36] the value of that in hovering flight, respectively.

A mesh convergence analysis was performed on the developed models with different numbers of elements to achieve a compro-

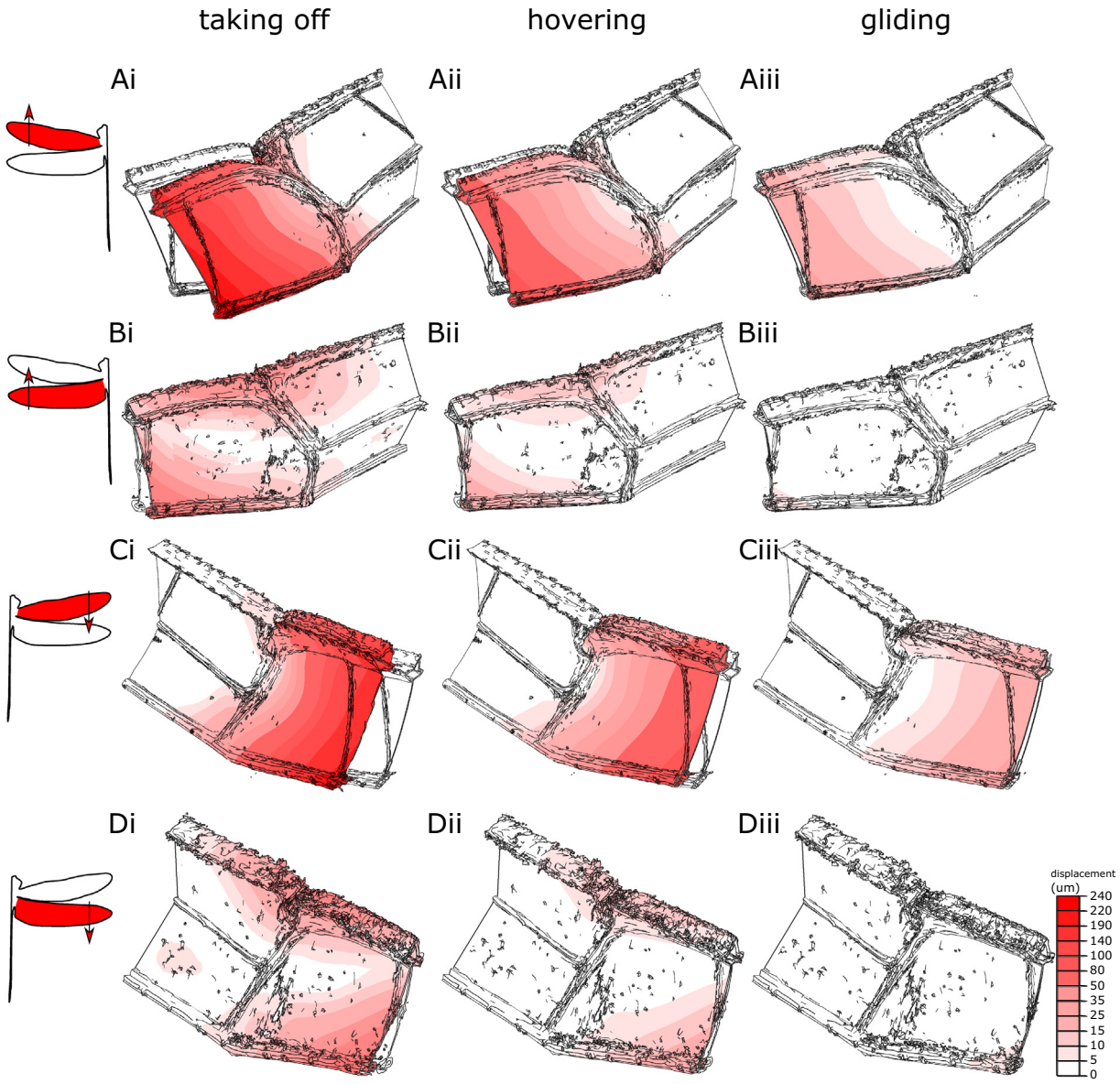

Fig. 4. Displacements of the (A, C) forewing and (B, D) hindwing nodi during the (A, B) up- and (C, D) downstrokes. The displacements are shown in three different flight modes: (Ai, Bi, Ci, Di) take-off, (Aii, Bii, Cii, Dii) hovering and (Aiii, Biii, Ciii, Diii) gliding. The models are shown from the (A, B) ventral and (C, D) dorsal sides when presenting the displacements in the up- and downstrokes, respectively. In order to give a better impression of the displacements both deformed and undeformed shapes are shown. All models are fixed at the extreme proximal edge and the maximum displacement occurs at their extreme distal edge.

Please cite this article in press as: H. Rajabi et al., Dragonfly wing nodus: A one-way hinge contributing to the asymmetric wing deformation, Acta Biomater. (2017), http://dx.doi.org/10.1016/j.actbio.2017.07.034

mise between the accuracy of the results and the computational time. It was found that a total number of elements of about 90,000 is needed for both fore- and hindwing nodus models to obtain the results which are not dependent on the mesh size.

3. Results

SEM images representing the 3D configuration of the fore- and hindwing nodi of the dragonfly *B. contaminata* are given in Fig. 2. Fig. 2A, B compares the geometry of the forewing nodus on the dorsal side with that on the ventral side. It seems that on both sides the costal vein (C) bends at the nodus and fuses to the posterior subcostal vein (ScP). The subcostal vein ends at the nodus on the dorsal side (Fig. 2A), but on the other side it appears to make a transition to the post-nodal part (Fig. 2B). A clear break can be observed between the pre-nodal and post-nodal parts, on the dorsal side of the forewing nodus (Fig. 2A). This break also exists on the ventral side (Fig. 2B), but it is less pronounced than that on the dorsal side. The nodus from the hindwing is seen to have almost the same characteristics as those already mentioned for the forewing nodus (Fig. 2C, D).

There is an elevated ridge on the dorsal sides of both fore- and hindwing nodi, which is absent on their ventral sides (see white arrows in Fig. 2A, C). The ridges on both wings are located on the distal end of the pre-nodal costal vein and they seem to partially cover the proximal part of the costal vein in the post-nodal region. A slight difference can be noted between the shapes of the ridges in the fore- and hindwing nodi. The elevated ridge of the hindwing appears to be a bit more bent, compared with that of the forewing (Fig. 2A, C). This difference can also be seen in the images taken by the CLSM (Fig. 3A, C).

The results from the CLSM analyses, illustrated in Fig. 3, reveal the presence of resilin-dominated areas in the cuticle of the wing nodus. These regions can be identified by their blue colour resulting from the blue autofluorescence of resilin [25]. Although resilin can be found on both sides of the nodi, its presence is more prominent on the ventral side (Fig. 3B, D) than on the other side (Fig. 3A, C). On the dorsal side, resilin is located at the interval of the pre- and post-nodal regions, and especially in the transition zone between the costal and subcostal veins (see arrows in Fig. 3A, C). On the ventral side, however, resilin spreads over a wider area, including the distal end of the pre-nodal costal vein (see arrows in Fig. 3B, D) and the interval of the pre- and post-nodal parts. Considering the relatively larger distance between the costal and subcostal veins in the forewing than in the hindwing (almost 1.33 times), the resilin-dominated area in the former is a bit more elongated. A good agreement was found between the results of the WFM and those of the CLSM, which supports the observations mentioned earlier (for more details on WFM data see Fig. S1).

Fig. 4 compares the displacements of the fore- and hindwing nodi during the up- and downstrokes in three different flight modes including take-off, hovering and gliding. The models are shown from the ventral and dorsal sides when presenting the results of the up- (Fig. 4A, B) and downstrokes (Fig. 4C, D), respectively. In order to provide a better impression of the displacements, both deformed and undeformed shapes of the models are given in this figure (the undeformed shapes remained uncoloured). The results indicate a clear difference between the displacements of the fore- and hindwing nodi. The displacement of the forewing nodus in this region seems to be a combination of both bending and twisting (Fig. 4A, C). However, in contrast, the hindwing nodus undergoes pure torsion (Fig. 4B, D). The magnitude of the displacements, however, considerably differs among the flight modes. As it was expected, the largest and smallest displacements occur during take-off and gliding flight, respectively. In the forewing nodus, the translational displacement in take-off is seen to be 2.2–2.4 and 7.8–8.2 times larger than those in hovering and gliding, respectively (Fig. 4A, C). These values are somewhat higher when comparing the angles of rotation in these three flight modes (2–2.8:1 and 6.7–17.8:1, respectively) (Fig. 4B, D). Taking into account that there is no bending in the hindwing nodus, the rotation of this model in take-off during the up- and downstrokes are measured to be 2.2–2.5 and 6.2–8.1 times larger than those in hovering and gliding, respectively (Fig. 4B, D). Table S1 lists the translational and rotational displacements of the fore- and hindwing nodi during the up- and downstrokes in all the studied flight modes.

An interesting phenomenon is observed when investigating the displacements of the models in hovering and take-off. After some levels of deformation, a contact occurs between the post-nodal costal vein and the elevated ridge on the pre-nodal costal vein. Video 1 shows the occurrence of this contact in the forewing nodus. In contrast, Video 2 represents the deformation of the same model when no contact pair is defined between the interacting surfaces. As can be seen here, the latter leads to a displacement which is almost 1.5 times larger than that of the former analysis. The displacement scale factor in both these videos is set to 2 to clearly show the difference in the deformation of the models. It is important to mention that the contact between the pre-nodal and post-nodal parts of the nodus is formed in both fore- and hindwings, but only during the downstroke. Video 3 presents the displacement of the forewing nodus in the upstroke. The legend and displacement scale factor were adjusted to be the same as those used in Video 1.

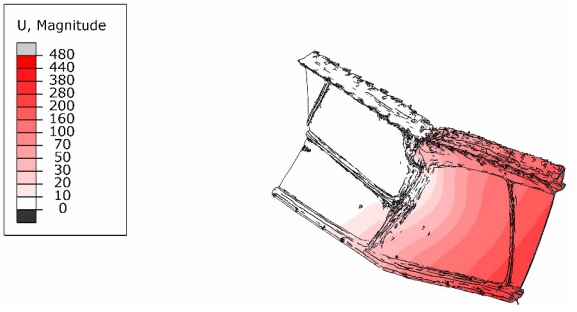

Video 1. Displacement of the forewing nodus when subjected to aerodynamic pressure on the ventral side (downstroke) during take-off. The video shows the formation of a contact between the costal vein in the distal part and the elevated ridge in the pre-nodal part of the forewing nodus resulting in an interlocking mechanism. The interlocking avoids further displacement of the nodus. Taking into account that the interlocking takes place only in the downstroke, it leads to dorso-ventral asymmetric deformation of the nodus. Displacement scale factor: 2.

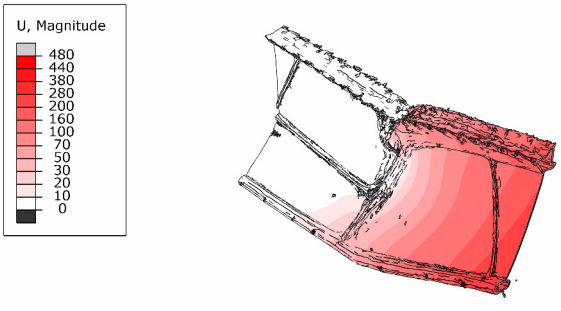

Video 2. Displacement of the same model used in Video 1 when no contact pair is defined between the interacting surfaces. This leads to an unrealistic large deformation, which is avoided by the interlocking mechanism of the real nodus. Displacement scale factor: 2.

Please cite this article in press as: H. Rajabi et al., Dragonfly wing nodus: A one-way hinge contributing to the asymmetric wing deformation, Acta Biomater. (2017), http://dx.doi.org/10.1016/j.actbio.2017.07.034

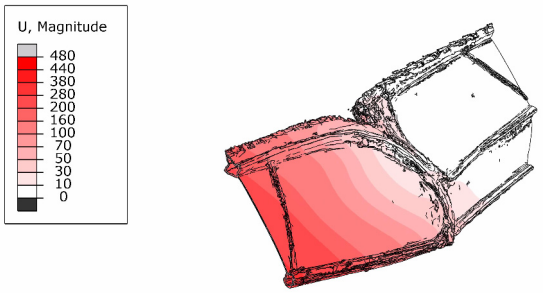

Video 3. Displacement of the forewing nodus when subjected to aerodynamic pressure on the dorsal side (upstroke) during take-off. Comparison of the displacements of the model given in this video and in Video 1 clearly shows the dorsoventral asymmetry of the nodus deformation. This asymmetric deformation is highly likely to be the result of the interlocking mechanism, which works only in the downstroke. Displacement scale factor: 2.

Fig. 5 shows the effect of the removal of resilin on the mechanical behaviour of the nodus. The figure compares the displacement and stress pattern of the realistic forewing nodus (Fig. 5A, C) with that of a similar model, but containing no resilin (Fig. 5B, D). In the second model, the resilin dominated areas are substituted by cuticle. Both models are subjected to the same aerodynamic pressures on their ventral sides (downstroke) during hovering flight. It is found that the removal of resilin decreases both translational and rotational displacements of the nodus by about 3 and 1.6 times, respectively (Fig. 5A, B). Looking at the stress distribution within the models, it can be noticed that in the realistic model the stress is mainly distributed on the post-nodal costal and anterior radial (R) veins (Fig. 5C). In contrast, in the other model the stress is particularly concentrated on the posterior subcostal vein and at the interval of the pre-nodal and post-nodal costal veins (see the black arrow in Fig. 5D).

4. Discussion

Previous studies have indicated a considerable difference in the deformability of fore- and hindwings in dragonflies [37,38]. One might expect this difference to arise from the different wing morphologies. In this study, however, we have seen that small geometric and material differences between the forewing and hindwing nodi result in different deformation patterns of this wing component (Fig. 4). These results are significant, since they suggest that, not only macroscopic differences, but even small changes in microscopic features of wing components may strongly influence their functionality. Any difference between the functionality of similar structural elements of fore- and hindwings can consequently result in different deformation patterns of the wings.

Our computational results showed the formation of contact between different parts of the wing nodus (Video 1). This contact formation, resulting in an interlocking mechanism, was found to operate when the wing is subjected to displacements larger than those exerted in gliding flight. Hence, it is likely that this mechanism is a design strategy to avoid extremely large displacements in the nodus. This is in accordance with the observations of Chen et al. [39] indicating the limited displacement of the nodus in the wings of the dragonfly *Sympetrum flaveolum*. However, one should take into account that this interlocking occurs only in one direction when the wing is subjected to forces on the ventral side (during the downstroke). Due to the absence of the elevated ridge on the other

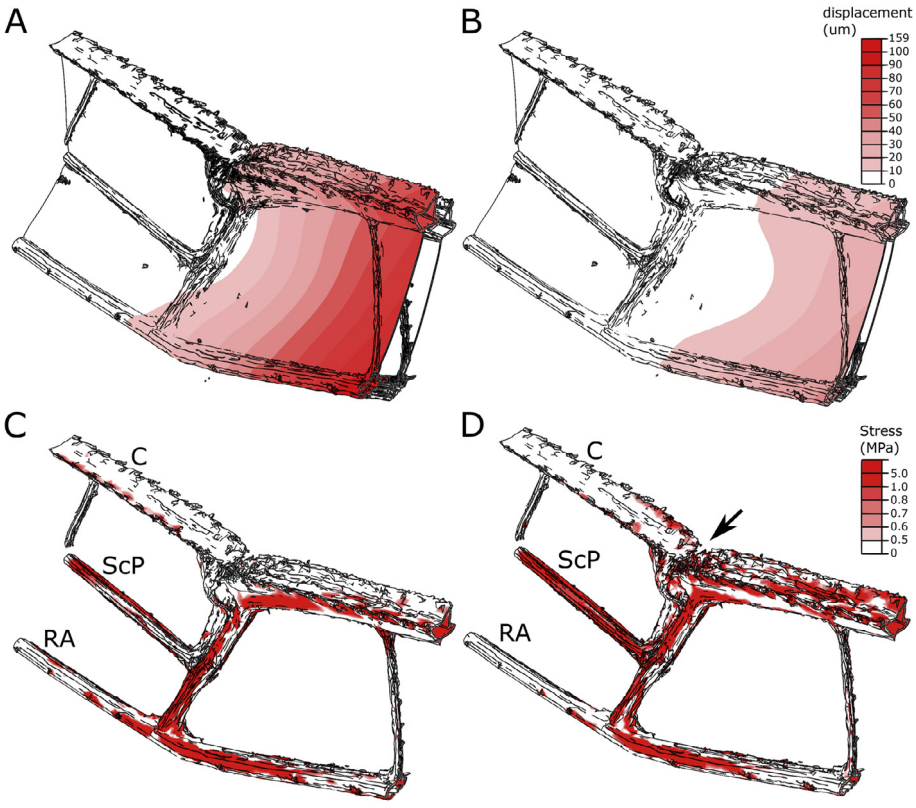

Fig. 5. Effect of the removal of resilin on the mechanical behaviour of the nodus. Displacements of the forewing nodus (A) before and (B) after removal of resilin. Distribution of maximum principal stress within the veins of the nodus (C) before and (D) after removal of resilin. The models are subjected to aerodynamic forces on their ventral sides in hovering flight.

Please cite this article in press as: H. Rajabi et al., Dragonfly wing nodus: A one-way hinge contributing to the asymmetric wing deformation, Acta Biomater. (2017), http://dx.doi.org/10.1016/j.actbio.2017.07.034

side (Figs. 2 and 3), the nodus is free to move in the other direction (Video 3). This geometric difference results in formation of a specialized "one-way" hinge, which allows the free movements in the upstroke and restrains the displacements in the downstroke (asymmetric displacements). Considering that the legend in Fig. 4 was chosen to cover a wide range of displacements and cannot adequately represent this asymmetry, we have updated the legend in Fig. 6. The displacements of the forewing nodus subjected to forces on the dorsal and ventral sides during take-off are represented in this image.

The asymmetric displacement of the nodus shown in Fig. 6 is expected to contribute to the observed dorso-ventral asymmetry in the displacement of dragonfly wings [40]. The wings are known to have an increased structural stiffness, and therefore an enhanced load bearing capacity, when they are subjected to aerodynamic forces in the downstroke. Taking into account that dragonflies generate most of their aerodynamic lift during the downstroke, the wing asymmetric displacement has been suggested to remarkably influence lift generation [41]. But, if the insect wings need this increased stiffness to resist external forces in flight, what role does resilin play in the nodus?

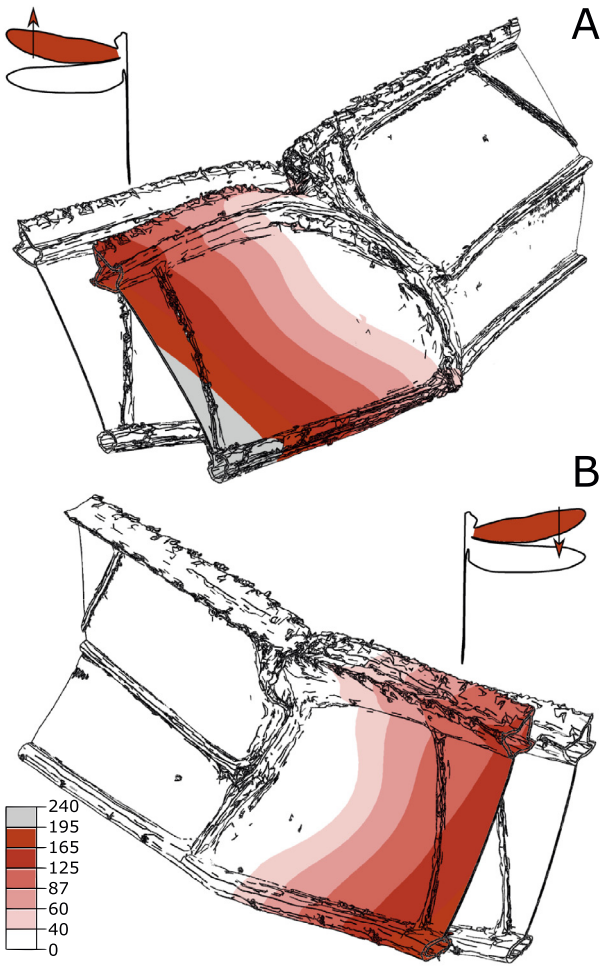

Fig. 6. Displacements of the forewing nodus in the (A) up- and (B) downstrokes during take-off. The models are shown from the (A) ventral and (B) dorsal sides when presenting the displacements in the up- and downstrokes, respectively. The interlocking mechanism of the nodus avoids further displacement of its distal part in the downstroke. This effect results in a dorso-ventral asymmetry in the deformation of the nodus. Here, the maximum displacement of the model in the upstroke is almost 1.5 times larger than that in the downstroke.

During the downstroke, the post-nodal part of the leading edge in both fore- and hindwing nodi was observed to experience a nose-down rotation (Fig. 4C, D). The rotation of the leading edge, resulting in twisting of the whole wing structure, has already been reported for the wings of several insect species [19,42]. This has been shown to remarkably improve the camber formation, and therefore the lift generation by dragonfly wings. Although there are some other structural components which are believed to contribute to wing twisting in flight [9,20,43], our numerical simulations suggest that the presence of resilin in the nodus may remarkably facilitate it. This assertion may be verified by the results illustrated in Fig. 5, indicating that the removal of resilin from the forewing nodus leads to a noticeably smaller rotation of the leading edge, compared to when resilin is present. However, both bending and twisting are required to a limited extent. The large deformations caused by further displacement of the wings subjected to external forces in flight are highly likely to negatively influence lift generation. As already mentioned, this is the role of the interlocking mechanism in the nodus to avoid these undesirable displacements, especially in the leading edge spar which is known to provide support for the whole wing structure.

On the other hand, our results indicated that the removal of resilin from the nodus transmits the stress from the costal and radial veins to the subcostal vein and the break in the costal vein (Fig. 5C, D). In contrast to the costal and radial veins, the subcostal vein is considerably thin and probably less strong. The discontinuity of the costal vein, forming the nodus, may also be considered as a critical zone. Previous studies have suggested that this part of the wing usually fails prior to any other wing region when subjected to high mechanical stresses [44]. Hence, one can conclude that the removal of the resilin may remarkably increase the possibility of the nodus failure. Taking into account that the wings have to withstand millions of cycles of mechanical loading during the lifespan of the insect, any damage in the wings is likely to decrease their fatigue resistance.

Future studies are planned to explore the possible variability of the structural and material characteristics of the nodus in various groups of Odonata to provide further insights into the functionality of this wing component depending on typical flight behaviour in different species.

Ethics

This work complies with ethical guidelines at Kiel University.

Conflicts of interest statement

The authors declare there are no conflicts of interest to disclose.

Funding

This study was financially supported by the Federal State Funding at Kiel University to HR.

Acknowledgements

The authors would like to thank Dr. Jan Michels (Kiel University) for his technical help and useful comments regarding confocal laser scanning microscopy. We also thank Dr. Sebastian Büsse for his kind assistance with micro-CT scanning.

Author contributions

HR, EA and SNG designed the study; HR, EA and SNG coordinated the study; HR, NG and KS conducted the research and analysed

the data; HR wrote the manuscript. HR, NG, KS, EA and SNG reviewed the manuscript, discussed the results and gave the final approval for publication.

Appendix A. Supplementary data

The FE models can be made available on request: please contact HR at hrajabi@zoologie.uni-kiel.de, harajabi@hotmail.com. Supplementary data associated with this article can be found, in the online version, at http://dx.doi.org/10.1016/j.actbio.2017.07.034.

References

[1] N.E. Carey, J.J. Ford, J.S. Chahl, Biologically inspired guidance for motion camouflage, in: Proceedings of the 5th Asian Control Conference (IEEE/IFAC-ASCC 2004), Melbourne, 2004.
[2] P.S. Corbet, Dragonflies: Behaviour and Ecology of Odonata, Harley Books, Colchester, 1999.
[3] D.J. Newman, The functional wing morphology of some Odonata (Doctoral Dissertation), University of Exeter, Exeter, 1982.
[4] R.J. Wootton, The functional morphology of the wings of Odonata, Adv. Odonatol. 5 (1991) 153–169.
[5] R.J. Wootton, Functional morphology of insect wings, Annu. Rev. Entomol. 37 (1992) 113–140.
[6] E. Appel, L. Heepe, C.P. Lin, S.N. Gorb, Ultrastructure of dragonfly wing veins: composite structure of fibrous material supplemented by resilin, J. Anat. 227 (2015) 561–582.
[7] S.N. Gorb, Serial elastic elements in the damselfly wing: mobile vein joints contain resilin, Sci. Nat. 86 (1999) 552–555.
[8] H. Rajabi, M. Rezasefat, A. Darvizeh, J.H. Dirks, Sh. Eshghi, A. Shafiei, T.M. Mostofi, S.N. Gorb, A comparative study of the effects of constructional elements on the mechanical behaviour of dragonfly wings, Appl. Phys. A 122 (2016) 1–13.
[9] H. Rajabi, N. Ghoroubi, A. Darvizeh, E. Appel, S.N. Gorb, Effects of multiple vein microjoints on the mechanical behaviour of dragonfly wings: numerical modelling, R. Soc. Open Sci. 3 (2016) 150610.
[10] R.J. Wootton, D.J. Newman, Evolution, diversification, and mechanics of dragonfly wings. Dragonflies & damselflies, in: A. Cordoba-Aguilar (Ed.), Model Organisms for Ecological and Evolutionary Research, Oxford University Press, Oxford, 2008, pp. 261–275.
[11] S.A. Combes, T.L. Daniel, Flexural stiffness in insect wings I. Scaling and the influence of wing venation, J. Exp. Biol. 206 (2003) 2979–2987.
[12] R.J. Wootton, K.E. Evans, R. Herbert, C.W. Smith, The hind wing of the desert locust (*Schistocerca gregaria* Forskal) I. Functional morphology and mode of operation, J. Exp. Biol. 203 (2000) 2921–2931.
[13] H. Rajabi, N. Ghoroubi, A. Darvizeh, J.H. Dirks, E. Appel, S.N. Gorb, A comparative study of the effects of vein-joints on the mechanical behaviour of insect wings: I. Single joints, Bioinspir. Biomim. 10 (2015) 056003.
[14] H. Rajabi, A. Shafiei, A. Darvizeh, S.N. Gorb, Resilin microjoints: a smart design strategy to avoid failure in dragonfly wings, Sci. Rep. 6 (2016) 39039.
[15] M. Vanella, T. Fitzgerald, S. Preidikman, E. Balaras, B. Balachandran, Influence of flexibility on the aerodynamic performance of a hovering wing, J. Exp. Biol. 212 (2009) 95–105.
[16] R.J. Wootton, Support and deformability in insect wings, J. Zool. 193 (1981) 447–468.
[17] E. Appel, S.N. Gorb, Comparative Functional Morphology of Vein Joints in Odonata, Zoologica, Schweizerbart Science Publishers, Stuttgart, 2014.
[18] S. Donoughe, J.D. Crall, R.A. Merz, S.A. Combes, Resilin in dragonfly and damselfly wings and its implications for wing flexibility, J. Morphol. 272 (2011) 1409–1421.
[19] A.R. Ennos, The importance of torsion in the design of insect wings, J. Exp. Biol. 140 (1988) 137–160.
[20] H. Rajabi, N. Ghoroubi, M. Malaki, A. Darvizeh, S.N. Gorb, Basal complex and basal venation of Odonata wings: structural diversity and potential role in the wing deformation, PLoS One 11 (2016) e0160610.
[21] H. Rajabi, A. Shafiei, A. Darvizeh, J.H. Dirks, E. Appel, S.N. Gorb, Effect of microstructure on the mechanical and damping behaviour of dragonfly wing veins, R. Soc. Open Sci. 3 (2016) 160006.
[22] R.Å. Norberg, Hovering flight of the dragonfly *Aeschna juncea* L., kinematics and aerodynamics, in: T.Y.-.T. Wu, C.J. Brokaw, C. Brennen (Eds.), Swimming and Flying in Nature, Plenum Press, New York, 1975.
[23] S. Fauziyah, C. Alam, R.C.H. Soesilohadi, B. Retnoaji, P. Alam, Morphological and mechanical characterisation of the hindwing nodus from the Libellulidae family of dragonfly (Indonesia), Arthropod. Struct. Dev. 43 (2014) 415–422.
[24] S.O. Andersen, T. Weis-Fogh, Resilin: a rubberlike protein in arthropod cuticle, Adv. Insect Physiol. 2 (1964) 1–65.
[25] J. Michels, S.N. Gorb, Detailed three-dimensional visualization of resilin in the exoskeleton of arthropods using confocal laser scanning microscopy, J. Microsc. 245 (2012) 1–16.
[26] S. Zill, S.F. Frazier, D. Neff, L. Quimby, M. Carney, R. DiCaprio, J. Thuma, M. Norton, Three-dimensional graphic reconstruction of the insect exoskeleton through confocal imaging of endogenous fluorescence, Microsc. Res. Tech. 48 (2000) 367–384.
[27] J. Michels, E. Appel, S.N. Gorb, Functional diversity of resilin in Arthropoda, Beilstein J. Nanotechnol. 7 (2016) 1241–1259.
[28] S.O. Andersen, Characterization of a new type of cross-linkage in resilin, a rubber-like protein, Biochim. Biophys. Acta 69 (1963) 249–262.
[29] H. Peisker, J. Michels, S.N. Gorb, Evidence for a material gradient in the adhesive tarsal setae of the ladybird beetle *Coccinella septempunctata*, Nat. Commun. 4 (2013) 1661.
[30] ABAQUS v6.7, Analysis User's Manual, Simulia, Providence, 2007.
[31] H. Rajabi, A. Darvizeh, A. Shafiei, D. Taylor, J.H. Dirks, Numerical investigation of insect wing fracture behavior, J. Biomech. 48 (2015) 89–94.
[32] H. Rajabi, P. Bazargan, A. Pourbabaei, Sh. Eshghi, A. Darvizeh, S.N. Gorb, D. Taylor, J.H. Dirks, Wing cross veins: an efficient biomechanical strategy to mitigate fatigue failure of insect cuticle, Biomech. Model. Mechanobiol. 16 (2017) 1–9.
[33] J.H. Dirks, D. Taylor, Fracture toughness of locust cuticle, J. Exp. Biol. 215 (2012) 1502–1508.
[34] S.R. Jongerius, D. Lentink, Structural analysis of a dragonfly wing, Exp. Mech. 50 (2010) 1323–1334.
[35] J.H. Marden, Maximum lift production during takeoff in flying animals, J. Exp. Biol. 130 (1987) 235–258.
[36] J.M. Wakeling, C.P. Ellington, Dragonfly flight. I. Gliding flight and steady-state aerodynamic forces, J. Exp. Biol. 200 (1997) 543–556.
[37] C. Koehler, Z. Liang, Z. Gaston, H. Wan, H. Dong, 3D reconstruction and analysis of wing deformation in free-flying dragonflies, J. Exp. Biol. 215 (2012) 3018–3027.
[38] H. Wang, L. Zeng, H. Liu, C. Yin, Measuring wing kinematics, flight trajectory and body attitude during forward flight and turning maneuvers in dragonflies, J. Exp. Biol. 206 (2003) 745–757.
[39] Y.H. Chen, M. Skote, Y. Zhao, W.M. Huang, Dragonfly (*Sympetrum flaveolum*) flight: kinematic measurement and modelling, J. Fluids Struct. 40 (2013) 115–126.
[40] S.A. Combes, T.L. Daniel, Flexural stiffness in insect wings II. Spatial distribution and dynamic wing bending, J. Exp. Biol. 206 (2003) 2989–2997.
[41] R.J. Wootton, R.C. Herbert, P.G. Young, K.E. Evans, Approaches to the structural modelling of insect wings, Philos. Trans. R. Soc. B 358 (2003) 1577–1587.
[42] A.R. Ennos, Comparative functional morphology of the wings of Diptera, Zool. J. Linn. Soc. 96 (1989) 27–47.
[43] R.J. Wootton, J. Kukalová-Peck, D.J.S. Newman, J. Muzón, Smart engineering in the mid-carboniferous: how well could Palaeozoic dragonflies fly?, Science 282 (1998) 749–751
[44] H. Rajabi, A. Darvizeh, Experimental investigations of the functional morphology of dragonfly wings, Chin. Phys. B 22 (2013) 088702.

Please cite this article in press as: H. Rajabi et al., Dragonfly wing nodus: A one-way hinge contributing to the asymmetric wing deformation, Acta Biomater. (2017), http://dx.doi.org/10.1016/j.actbio.2017.07.034